JOURNAL OF MATERIALS SCIENCE 27 (1992) 1317–1321

Evolution of 2223 phase in the $Bi_2Pb_{0.6}Sr_2Ca_2Cu_{3.1}O_y$ system

B. GOGIA, S. C. KASHYAP, D. K. PANDYA, K. L. CHOPRA
Thin Film Laboratory, Department of Physics, Indian Institute of Technology, New Delhi 110 016, India

The role of cationic ratios (Sr/Ca and Bi/Pb) in the evolution of high-T_c phase (2223) in samples prepared under different sintering conditions, starting with a composition of $Bi_2Pb_{0.6}Sr_2Ca_2Cu_{3.1}O_y$ has been investigated by employing energy-dispersive X-ray analysis, scanning electron microscopy and X-ray diffraction. As manifested by the observed decrease in Sr/Ca ratio, an increase in sintering temperature from 822 to 852 °C increases the disorder in Sr–O and Ca layers. The observed increase in the volume fraction of 2223 phase and the contraction in *c*-axis parameter have been explained on the basis of the observed decrease in Sr/Ca ratio. It thus appears that the disorder caused by the intersubstitution of Ca and Sr in SrO and Ca layers and partial replacement of Bi by Pb in the structure promote the evolution and growth of 2223 phase.

1. Introduction

The Bi–cuprate system (BSCCO) was the first multiphasic superconducting system [1] exhibiting a zero-resistance transition temperature, T_c, exceeding 100 K. A. high-T_c phase with a composition of $Bi_2Sr_2Ca_2Cu_3O_y$ (2223) and T_c of 110 K is generally found to coexist with a low-T_c ($\sim$ 85 K) phase of composition $Bi_2Sr_2Ca_1Cu_2O_y$, (2212). Several efforts [2–9] have been made to stabilize the high-T_c 2223 phase. It is found that excess Cu [2] and/or both Ca and Cu [3–5] facilitate the evolution of 2223 phase. The addition of Pb to the BSCCO system facilitates the formation of 2223 phase by modifying the growth kinetics [6–9]. The resulting 2223 phase was observed to possess a cationic arrangement and ratios other than those expected from the stoichiometry, e.g. Bi on Sr/Ca sites [10], disorder in Sr and Ca layers [11–15], and Pb occupying Bi sites [10]. In view of this, investigations are still needed in order to clarify the role of this randomness of cationic arrangement in the evolution of 2223 phase from 2212 phase. To achieve this we have carried out a systematic study on the evolution of 2223 phase using the appropriate composition [16] under various sintering conditions.

Also in the present work, we emphasize the importance of microstructural investigations by scanning electron microscopy (SEM) and energy-dispersive X-ray analysis (EDX) in assessing the effect of sintering temperature on the cationic ratio of elements and their relation to the formation of 2223 phase, as such work is necessary when studying these multiphasic compounds comprising phases differing in thermal stability. To do this, compositional analyses were done at every step of processing using EDX. To further support these results, electrical and structural properties were also exploited.

2. Experimental procedure

The samples were prepared by the solid-state reaction of Bi_2O_3, PbO, $SrCO_3$, $CaCO_3$ and CuO powders. The ratio of elements Bi, Pb, Sr, Ca and Cu was 2:0.6:2:2:3.1. The powders were well mixed, calcined first at 800 °C for 20 h and then at 820 °C for 3 h with intermediate grindings and finally at 840 °C for 12 h. The pellets made were sintered in air in separate runs at 822, 842 or 852 °C for a period of 25, 50, 75, 100, 125, 150 or 175 h and were designated by a letter (B, C and D, respectively) followed by a number (1 to 7), e.g. sample C7 implies that sintering is carried out at 842 °C for 175 h. In each case the samples were cooled in O_2 down to 500 °C, where they were kept for 24 h before being finally furnace-cooled to room temperature.

Resistivity, ρ, and critical current density, J_c, measurements were done on rectangular bars by employing a d.c. four-probe method in zero applied magnetic field. The reaction products were analysed by using an X-ray diffractometer (Rigaku RU 200 B) and their microstructural analysis was carried out using a scanning electron microscope (Philips 525M). The chemical composition was analysed by an energy-dispersive X-ray analyser (Philips PV9900).

3. Results and discussion

3.1. Electrical properties

The results of resistivity measurements made in the temperature range 300 to 15 K are summarized in Table I. The variation of electrical resistivity of some typical samples, exhibiting the effect of sintering temperature and duration, is shown in Figs 1 and 2. In the case of samples belonging to set B (B1 and B7) no step in the resistivity curve close to 112 K, indicative of high-T_c phase, was seen even after sintering for 175 h. Rather, a broad transition with an onset, T_{co}, at 85 K

0022–2461

TABLE I Variation of transition temperature, T_{co} and T_c, and critical current density, J_c, with sintering temperature and duration

Sintering temperature (°C)	Sintering time (h)	Sample No.	T_c (K)	T_{co} (K)	J_c (at 77 K) (A cm^{-2})
822	25	B1	47	67	–
	50	B2	50	67	–
	100	B4	59	80	–
	175	B7	77	85	–
842	25	C1	50	70	–
	50	C2	55	70	–
	100	C4	103	110	70
	175	C7	107.5	112	96
852	25	D1	51	70	–
	50	D2	54	73	–
	75	D3	100	110	55
	100	D4	107	112	78
	125	D5	110	112	90
	150	D6	112	114	116
	175	D7	112	115	130

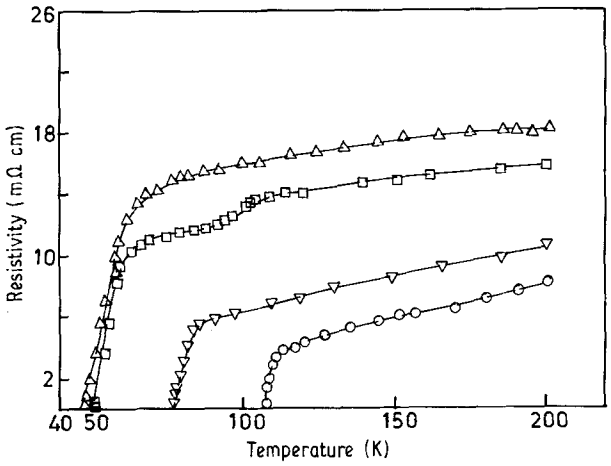

Figure 1 Resistivity versus temperature plots for samples of composition $Bi_2Pb_{0.6}Sr_2Ca_2Cu_{3.1}O_y$ sintered at 822 °C (denoted by B) and 842 °C (denoted by C) for (△) 25 h (B1), (□) 25 h (C1), (▽) 175 h (B7) and (○) 175 h (C7).

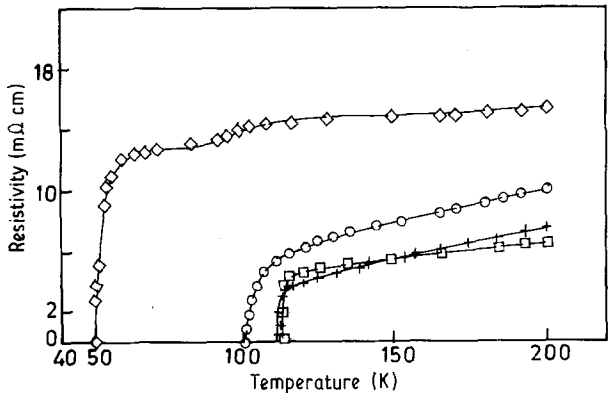

Figure 2 Resistivity versus temperature plots for samples of composition as in Fig. 1, sintered at 852 °C for (◇) 25 h (D1), (○) 75 h (D3), (+) 125 h (D5) and (□) 175 h (D7).

and a T_c of 77 K was seen in the latter sample. On the other hand, sample C1 (Fig. 1) showed a step in the resistivity curve around 100 K which vanished on further increase of sintering time beyond 50 h, and led

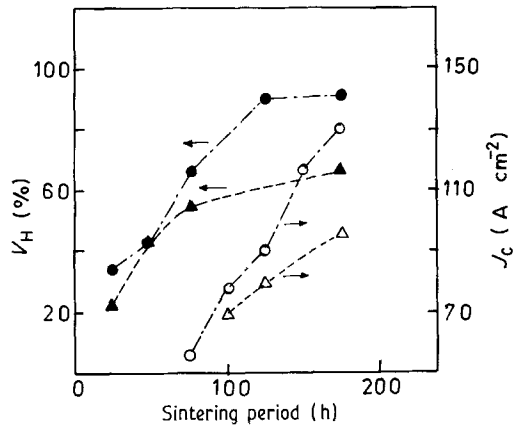

Figure 3 Variation of volume fraction of 2223 phase (V_H) and critical current density (J_c) with sintering temperature and period. (▲, △) Set C, (●, ○) set D, sintered at 842 and 852 °C, respectively.

to a single-step transition with a maximum T_c of 107.5 K and a transition width of 4.5 K (Fig. 1, C7).

Sample D1 (Fig. 2) showed a non-metallic behaviour exhibiting almost no variation in resistivity with temperature down to 100 K. A small drop close to this temperature is followed by a very low T_c of only 51 K (Table I). It is seen from the curves for samples D3, D5 and D7 that with increase of sintering time beyond 50 h the resistivity behaviour changed to metallic and only a single transition with a T_c of 110 and 112 K was observed with a ΔT_c of 2 and 3 K (Table I) for samples D5 and D7, respectively. Like the transition temperature, the critical current density, J_c, measured at 77 K was also enhanced with increase of sintering temperature and duration. It is evident from Table I and Fig. 3 that samples sintered at 852 °C exhibited a higher J_c at 77 K at all stages. A maximum value of 130 A cm^{-2} was observed for D7.

It is evident from the above electrical properties that with an increase of sintering temperature from 822 to 852 °C, the high-T_c phase nucleates with an improved grain connectivity which is responsible for a decrease of normal-state resistivity and improvement of both T_c and J_c. In order to establish a correlation

between the electrical properties and the different phases formed under varying sintering conditions, structural and microstructural investigations were done in all cases.

3.2. Phase identification through X-ray diffraction analysis

The analysis of X-ray diffractogram of the as-calcined powder revealed that the powder consisted primarily of the low-T_c phase (2 2 1 2). Small fractions of a lower-T_c phase (2 2 0 1), Ca_2PbO_4 and CuO were also present. The sintering at 822 °C of the pellets (set B) made from this powder resulted mainly in 2 2 1 2 phase along with a small fraction of 2 2 0 1 phase. Even prolonged heating (up to 175 h), did not produce any trace of 2 2 2 3 phase (Fig. 4, B7). The samples belonging to set C, however, showed the evolution of 2 2 2 3 phase. In addition, the other phases present were 2 2 1 2, 2 2 0 1, and traces of Ca_2PbO_4 and CuO. A large fraction of these reaction products transformed to 2 2 2 3 phase with increase of sintering time. The volume fraction of high-T_c phase, V_H (%), was estimated from the intensities of dominant and separated peaks of 2 2 2 3 (0 0 $\underline{2}$ $\underline{1}$), 2 2 1 2 (0 0 8) and 2 2 0 1 (0 0 8). It is seen that the fraction of 2 2 2 3 phase increased from 23% (C1) to a maximum of 66% for C7 (as shown in Fig. 3 for set C). The X-ray diffractogram of the same sample (C7) is shown in Fig. 4, C7. Similar to this case, the samples sintered at 852 °C showed the evolution of 2 2 2 3 phase after 25 h of sintering. However, the rate of growth was faster in this case, as evinced by the increase of volume fraction of 2 2 2 3 phase to 34% (D1) and 90% (D5). Sintering beyond 125 h, however, did not show any change until 175 h (Fig. 3, D).

The above structural investigations suggest that sintering at 822 °C was not adequate for the nucleation of 2 2 2 3 phase. With increase of temperature in the range of 842–852 °C, the 2 2 2 3 phase evolved from the 2 2 1 2 phase. This could be attributed to the diffusion of Ca and Cu from the Ca_2PbO_4 and CuO in the growing structure. The observed increase of T_c from 77 to 112 K as the sintering temperature was increased from 822 to 852 °C is understandably due to the evolution of enough 2 2 2 3 phase in 150 h.

With an increase in V_H in both sets of samples (C and D), the c-axis parameter contracted from 3.728 (C1) to 3.705 nm (C7) and from 3.705 (D1) to 3.675 nm (D5), respectively. The lattice parameters a and b were generally invariant throughout the process except in the first 50–75 h of sintering. Fig. 5 shows the variation of lattice parameter for the set D samples. The superconducting phases formed from different nominal compositions having different Ca contents have been reported to exhibit a reduction in c-axis parameter [2, 17] with an increase of Ca content in the starting composition. In the present case, however, a systematic contraction in c-axis parameter with the evolution of 2 2 2 3 phase (in both set C and set D) from the single starting composition was observed. The observed variation could be explained by proposing that there are changes in the cationic ratios of the elements, especially Ca and Sr, with the formation of 2 2 2 3 phase. To confirm the above proposal, microstructural and compositional analyses were also made.

3.3. Microstructural and compositional analyses

Some typical scanning electron micrographs of representative samples are shown in Fig. 6. It is clear from the micrograph of B7 (Fig. 6a) that crystallites of variable shapes and sizes are randomly distributed. The other samples of this batch showed a similar pattern. However, in the case of set C the crystallites were plate-like in shape and their size was found to increase with sintering time. Fig. 6b shows randomly oriented platelets of ~ 30 μm in a typical sample. With further

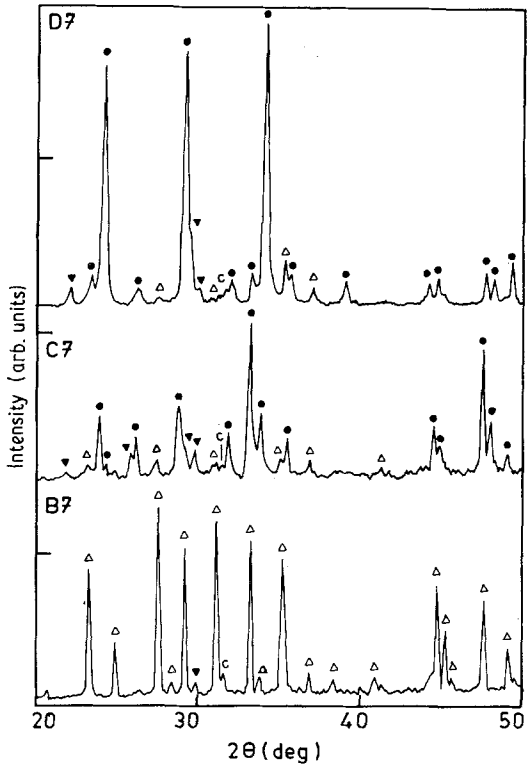

Figure 4 X-ray diffractograms of samples having compositions as in Fig. 1, sintered at 822 °C (B7), 842 °C (C7) and 852 °C (D7) for 175 h. (●) 2223, (△) 2212, (▼) 2201, (c) Ca_2PbO_4.

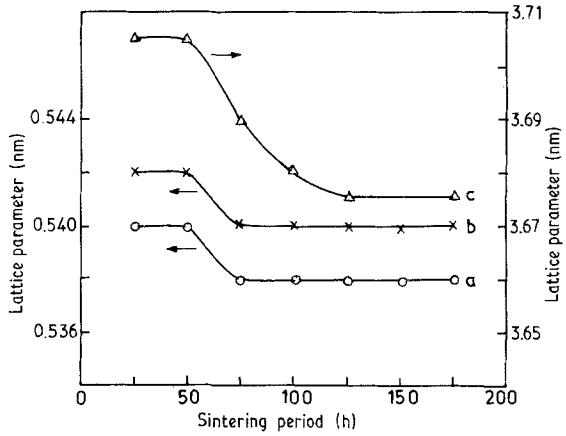

Figure 5 Variation of lattice parameters of samples of set D with sintering period.

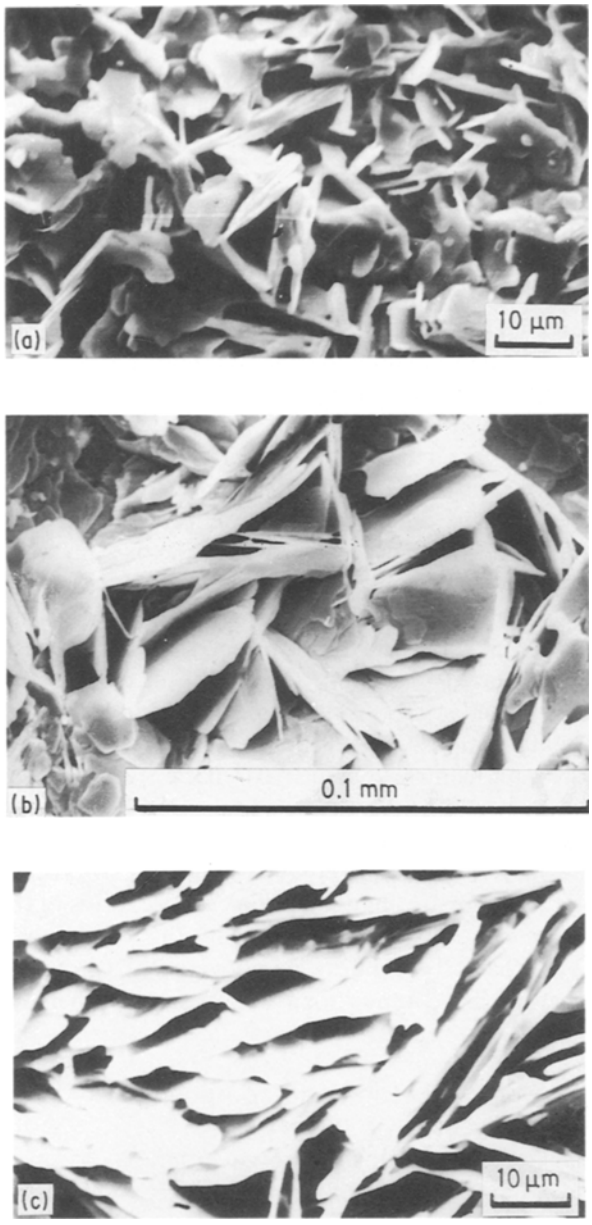

Figure 6 Scanning electron micrographs of samples (a) B7, (b) C7 and (c) D7 sintered at 822, 842 and 852 °C, respectively, for 175 h.

increase in sintering temperature, the platelet-size and orientation improved (Fig. 6c). The compactness of the structure in this case is responsible for the higher J_c of D7 compared with C7.

Chemical composition analysis, done in all cases, showed some interesting relations with the different phases formed. In the case of samples belonging to set B, the average elemental composition of a sample came out to be nearly 2:3:2 for Bi:(Sr, Ca):Cu, which is in conformity with the observed 2212 phase by using XRD (Fig. 4, B7) data.

It may be pointed out that in sample B1, the Ca content was higher (Sr/Ca $\approx$ 1.22) than the stochiometric requirement. This could be attributed to the intersubstitution of Ca and Sr, and more probably of Ca on Sr sites [11]. A change in this ratio was expected if there were any growth of 2223 phase. However, no appreciable change in the elemental ratio (Sr/Ca) was observed with further increase in sintering time of set B (Fig. 7). The lattice constants were also unchanged during this period.

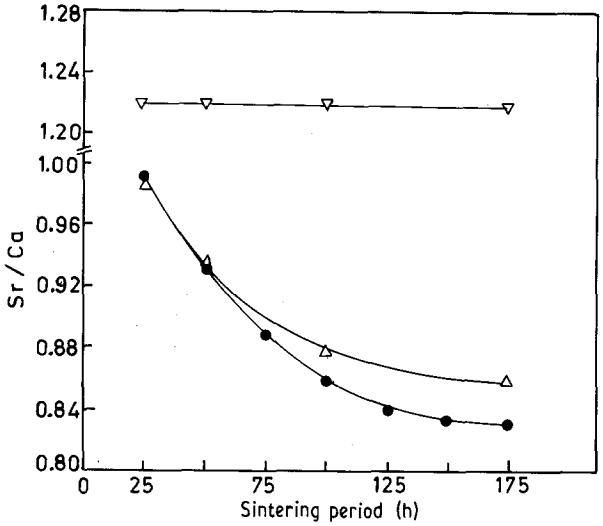

Figure 7 Variation of Sr/Ca ratio with sintering time of samples of starting composition $Bi_2Pb_{0.6}Sr_2Ca_2Cu_{3.1}O_y$, sintered at (▽) 822 °C (set B), (△) 842 °C (set C) and (●) 852 °C (set D).

Besides this, in the initial stages of sintering some features having shapes different from that of platelets were also observed (set B). A typical compositional analysis of such a region gave Ca and Pb in the ratio 2:1. This result, together with X-ray data, confirmed that these features correspond to Ca_2PbO_4. Prolonged heating caused the disappearance of such features. In comparison to set B, sintering in the other two sets (C and D) resulted in a more homogeneous product, as different regions exhibited the same ratio of elements within a limit of $\pm$ 1 at %. The change in Sr/Ca ratio with sintering time for the sets C and D is shown in Fig. 7. In both cases this ratio was always less than unity, a value which corresponds to the stochiometric high-T_c phase. It decreased from 0.99 (C1) to 0.86 (C7) and from 0.99 (D1) to 0.83 (D5) with increase in sintering duration.

This behaviour is identical to that of the increase in volume fraction of 2223 phase and contraction of c-axis parameter. A greater amount of Ca at the expense of Sr in the structure, however, suggested the possibility of Ca occupying Sr sites, thus leading to disorder in the SrO and Ca layers which probably helps in stabilization of the high-T_c phase. X-ray photoelectron spectroscopy studies [14, 15] also revealed an increase in disorder in these layers with enhancement of the volume fraction of high-T_c phase. Compositional analysis of leaded and lead-free samples prepared under identical conditions has shown a decrease in Bi content in leaded samples. X-ray photoelectron spectroscopic investigations have shown that nearly 10% of the Bi is replaced by Pb [15]. The observed contraction of a and b lattice parameters could therefore be attributed to the partial replacement of Bi^{3+} by Pb^{2+}.

4. Conclusion

In summary, an increase of sintering temperature from 822 to 852 °C for the composition $Bi_2Pb_{0.6}Sr_2Ca_2Cu_{3.1}O_y$ led to the evolution of high-T_c phase.

The increase in disorder in Sr–O and Ca layers and also the partial replacement of Bi by Pb in the layered structure at these temperatures assist in the stabilization of the high-T_c phase.

Acknowledgements

Financial support from CSIR and the help of Dr Chhatar Singh and Mr V. K. Khanna in EDX and SEM studies are gratefully acknowledged.

References

1. H. MAEDA, Y. TANAKA, M. FUKSUTUMI and T. ASANO, *Jpn J. Appl. Phys.* **27** (1988) L209.
2. G. CALESTANI, C. RIZZOLI, G. D. ANDREETTI, E. BULUGGIU, D. C. GIORI, A. VALENTI, A. VERA and G. AMORETTI, *Physica C* **158** (1989) 217.
3. N. KIJIMA, H. ENDO, J. TSUCHIYA, A. SUMIYAMA, M. MIZUNO and Y. OGURI, *Jpn J. Appl. Phys.* **27** (1988) 1852.
4. S. KOYAMA, U. ENDO and T. KAWAI, *ibid.* **27** (1988) L1861.
5. J. TSUCHIYA, H. ENDO, N. KIJIMA, A. SUMIYAMA, M. MIZUNO and Y. OGURI, *ibid.* **28** (1989) 1918.
6. S. A. SUNSHINE, T. SIEGRIST, L. F. SCHNEEMEYER, D. W. MURPHY, R. J. CAVA, B. BATLOGG, R. B. Van DOVER, R. M. FLEMING, S. H. GLARUM and S. NAKAHARA, *Phys. Rev. B* **38** (1989) 893.
7. M. MIZUNO, H. ENDO, J. TSUCHIYA, N. KIJIMA, A. SUMIYAMA and Y. OGURI, *Jpn J. Appl. Phys.* **27** (1988) L1225.
8. S. M. GREENE, C. JIANG, Y. MEI, H. L. LUO and C. POLITIS, *Phys. Rev. B* **38** (1988) 5016.
9. H. K. LIU, S. X. DOU, N. SAVVIDES, J. P. ZHOU, N. X. TAN, A. J. BOURDILLON, M. KVIZ and C. C. SORRELL, *Physica C* **157** (1989) 93.
10. R. RAMESH, M. S. HEGDE, C. C. CHENG, J. M. TARASCON, S. M. GREEN and H. L. LUO, *J. Appl. Phys.* **66** (1988) 4878.
11. R. G. BUCKLEY, J. L. TALLON, I. W. M. BROWN, M. R. PRESLAND, N. E. FLOWER, P. W. GILBERD, M. BOWDEN and N. B. MILESTONE, *Physica C* **156** (1988) 629.
12. E. AGOSTINELLI, J. BOHANDY, W. J. GREEN, C. B. BARGERON, T. E. PHILIPS, B. F. KIM, F. J. ADRIAN and K. MOORJANI, *J. Supercond.* **2** (1989) 361.
13. S. KOHIKI, T. WADA, S. KAWASHIMA, H. TAKAGI, S. UCHIDA and S. TANAKA, *Phys. Rev. B* **38** (1988) 8868.
14. D. K. RAI, A. K. SARKAR, T. N. WITTBERG and B. KUMAR, *J. Appl. Phys.* **66** (1989) 3950.
15. K. L. CHOPRA, D. BHATTACHARYA, P. PRAMANIK, S. C. KASHYAP, B. GOGIA, M. C. BHATNAGAR and D. K. PANDYA, in Proceeding of International Conference on Superconductivity, Bangalore, January 1990, edited by S. K. Joshi, C. N. R. Rao and S. V. Subramanyam (World Scientific, Singapore, 1990) p. 86.
16. B. GOGIA, S. C. KASHYAP, D. K. PANDYA and K. L. CHOPRA, *Solid State Commun.* **73** (1990) 573.
17. M. YOSHIDA, *Jpn J. Appl. Phys.* **27** (1988) L2044.

Received 13 December 1990
and accepted 13 May 1991